

Review on Stress Corrosion Cracking of Metals

150

(delayed hydride cracking), Ni

Zr-2.5Nb

(DHC)

100-300 °C

DHC

DHC

Ni

/

DHC

Abstract

The objective of this study is an understanding of stress corrosion cracking of metals that is recognized to mostly limit the lifetime of the structural materials by comparing the features of delayed hydride cracking of zirconium alloys with those of stress corrosion cracking (SCC) of Ni-based alloys and hydrogen cracking of stainless steels. To this end, we investigated a dependence of delayed hydride cracking (DHC) velocity on the applied stress intensity factor and yield strength, and correlated a temperature dependence of the striation spacing and the DHC velocity. We reviewed a similarity of the features between the DHC of zirconium alloys, the SCC of Ni-based alloys and turbine rotor steels, and the hydrogen cracking of stainless steels and discussed the SCC phenomenon in metals with our DHC model.

1.

가

,

가

,

가

.

,

Zr, T, V

, Ni

,

Cu

2

V

가

[1].

[1].

가

head

,

Ni

(

600

690, X-750)

50

가

,

가

1

,

[2].

hcp

, delayed hydride cracking

가

Zr-2.5Nb

delayed hydride cracking

가

[3].

DHC

, DHC

DHC

DHC

Ni

가

(DHC)

Ni

2.

70 delayed hydride cracking (DHC)

가 AECL

DHC

가 가

가

[4]. Dutton Puls

DHC [5,6].

DHC (1)

DHC

,

1

DHC , K_{app}

가

, K_{IH} (1)

가 K_{app} (II), K_{app}

2 Ambler [7]

가 DHC

가 DHC

가 가 DHC 가 DHC

180 °C 450K

가 DHC , DHC

가 DHC ,

가 DHC

DHC

DHC 3

(striation lines)

DHC 가

, 가 DHC

[8]. DHC

4

X-ray (5). DHC δ -Zr , {111} δ -DHC
 . 3 가 6
 , 가
 DHC 가
 . DHC 가
 (6).

3. (hydrogen cracking)

7 1960 가 K_H $K > K_H$ 가
 가
 1 DHC
 8-(a) (b) 18Ni maraging
 160 °C
 [9]. 9 Stachle가 Ni
 [10]. 7-9

DHC , 가 DHC

[8]. 10 가 [11]. 가 , 가
 . 11
 Cu acoustic emission count 가
 [12]. 12
 , 3

4.

, , Ni , Cu
3 : 1 가
, 2 가
가 가 가
3 가 가
2
, DHC (), Ni
DHC
Cu
DHC
, DHC
가 가

1. A. Zielinski, "Hydrogen Assisted Degradation of Some Non-Ferrous Metals and Alloys", J. Materials Processing and Technology 109 (2001) p. 206.
2. G.E. Kerns and R.W. Staehle, Scripta Met., 6, 631 (1972).
3. B.A. Cheadle, E.G. Price, "Operating Performance of CANDU Pressure Tubes", Atomic Energy of Canada Limited Report, AECL-9939, 1989.
4. C.E. Coleman and J.F.R. Ambler, "Delayed Hydrogen Cracking in Zr-2.5 wt.%Nb Alloy", Reviews on Coatings and Corrosion, 3, 105 (1979).
5. R. Dutton, K. Nuttal, M.P. Puls and L.A. Simpson, Metallurgical Transactions A, 8A, 1553 (1977).
6. M.P. Puls, L.A. Simpson and R. Dutton, in Fracture Problems and Solutions in the Energy Industry, L.A. Simpson, Ed., Pergamon Press, Oxford, 1982, pp. 13-25.
7. J.F.R. Ambler, in Zirconium in the Nuclear Industry: Sixth International Symposium, ASTM STP 824, D.G. Franklin and R.B. Adamson, Eds., American Society for Testing and Materials, Philadelphia, 1984, pp. 653-674.
8. Y.S. Kim et al, To be presented at the 14th Symposium on Zirconium in the Nuclear Industry to be held in June, 2004.

9. R.P. Gangloff and R.P. Wei, "Gaseous Hydrogen Embrittlement of High Strength Steels", Metallurgical Transactions A, 8A, 1043 (1977).
10. R.W. Staehle, "Initiation and Propagation of SCC in Inconels for Steam Generator Applications", The 2nd Seminar on Nuclear Materials and Related Technology, 6-1, 1996.
11. R.M. Magdowski and M.O. Speidel, "Clean Steels for Steam Turbine Rotors-Their Stress Corrosion Cracking Resistance", Metallurgical Transactions A, 19A (1988) p. 1583.
12. E.N. Pugh, "Progress Toward Understanding the Stress Corrosion Problem", Corrosion-NACE, 41 (1985) p.517.

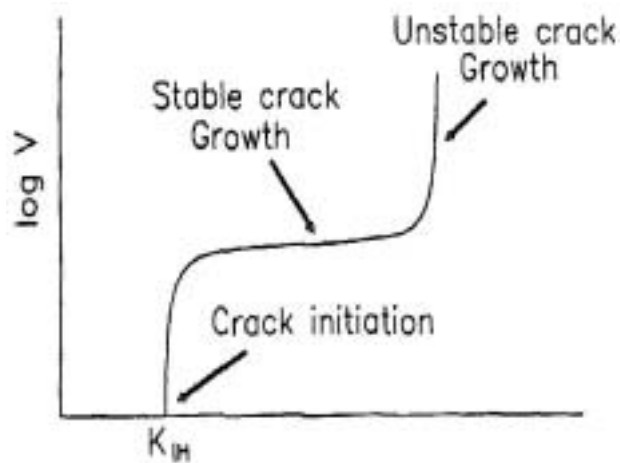


Fig. 1. Dependence of the crack growth velocity with applied stress intensity factor.

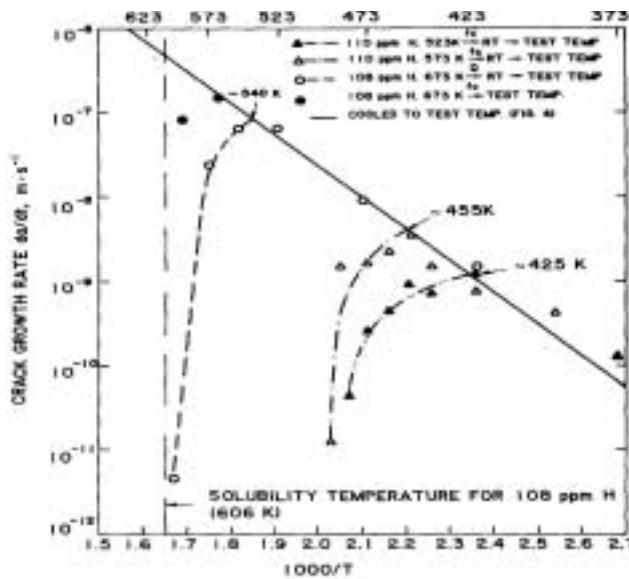


Fig. 2. Crack growth velocity of the Zr-2.5Nb tube with an approach to the test temperature by either heating-up or cool-down.

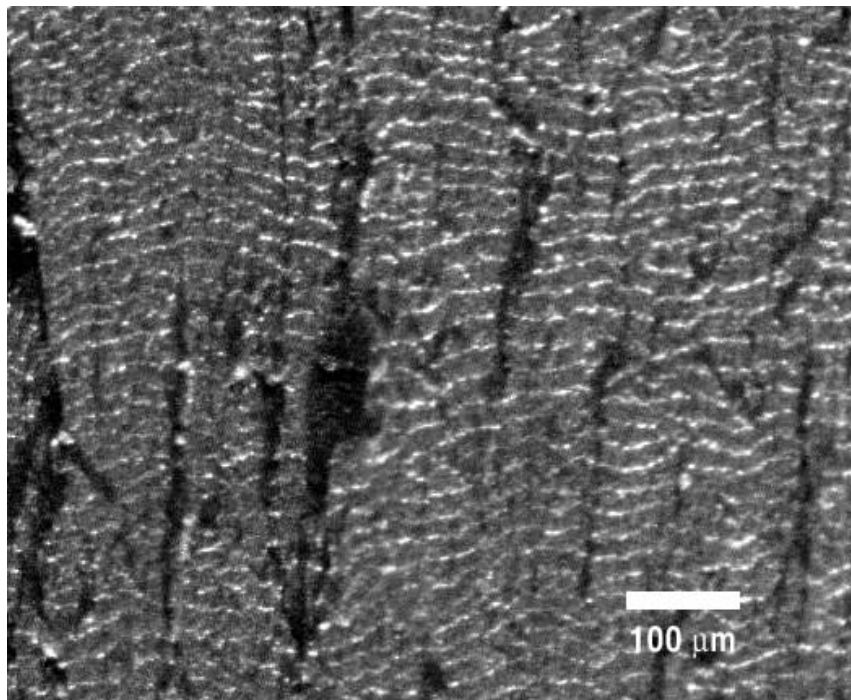
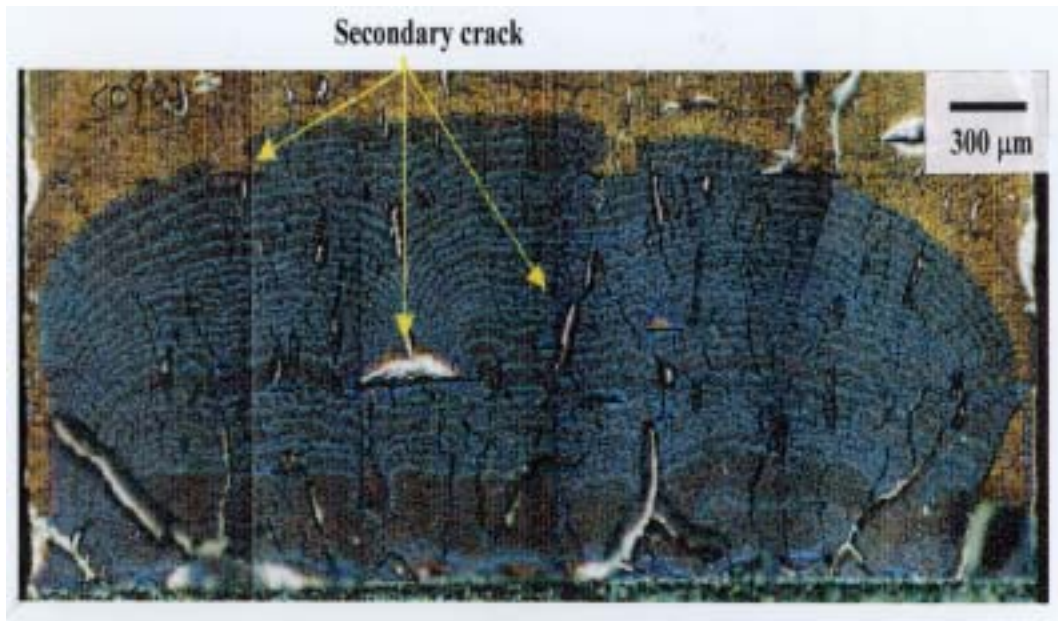


Fig. 3. Striation lines observed on the fractured surfaces of the Zr-2.5Nb tube after the DHC test.

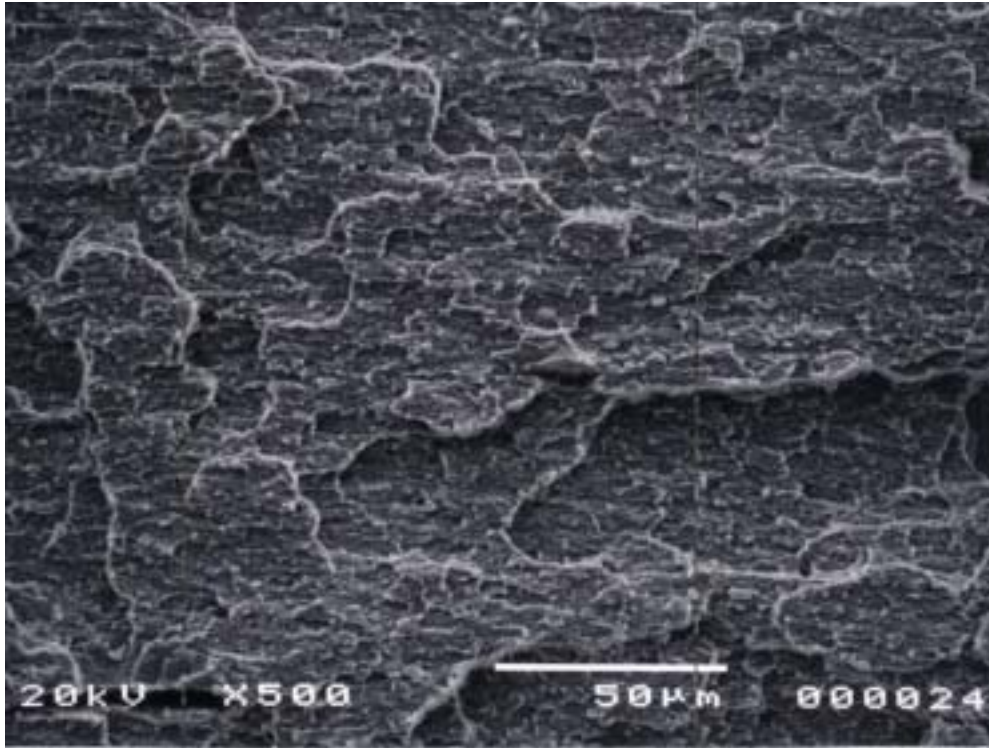


Fig. 4. Brittle fracture pattern observed on the DHC fractured surface of the Zr-2.5Nb tube.

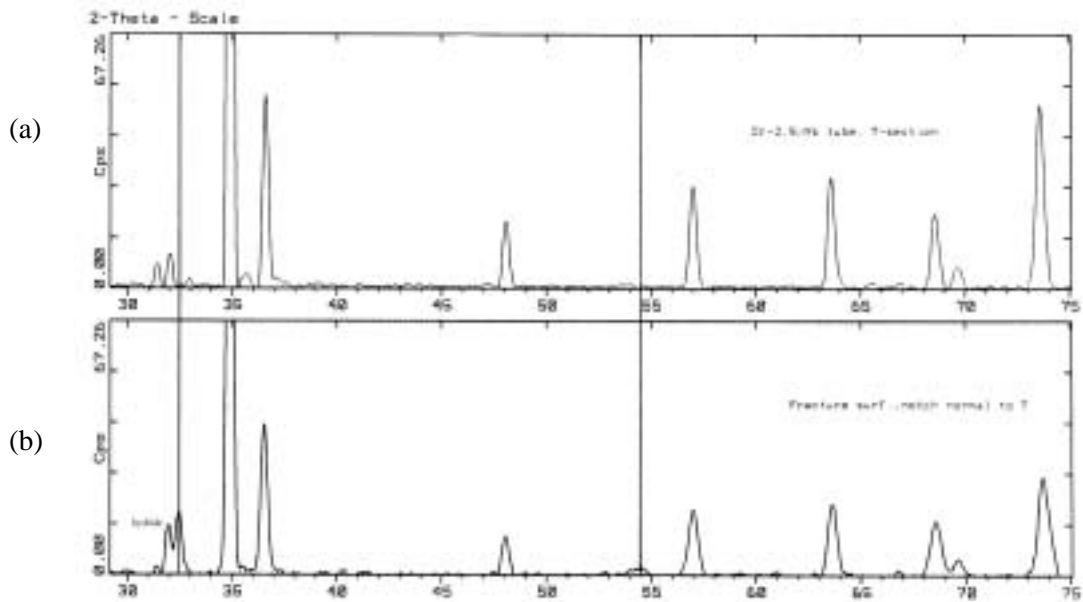


Fig. 5. XRD patterns determined (a) at a distance of 20 mm from the fractured surface and (b) at the fractured surface of L90 CB specimen after DHC testing at 250 °C, demonstrating the hydrides sitting on the fractured surface.

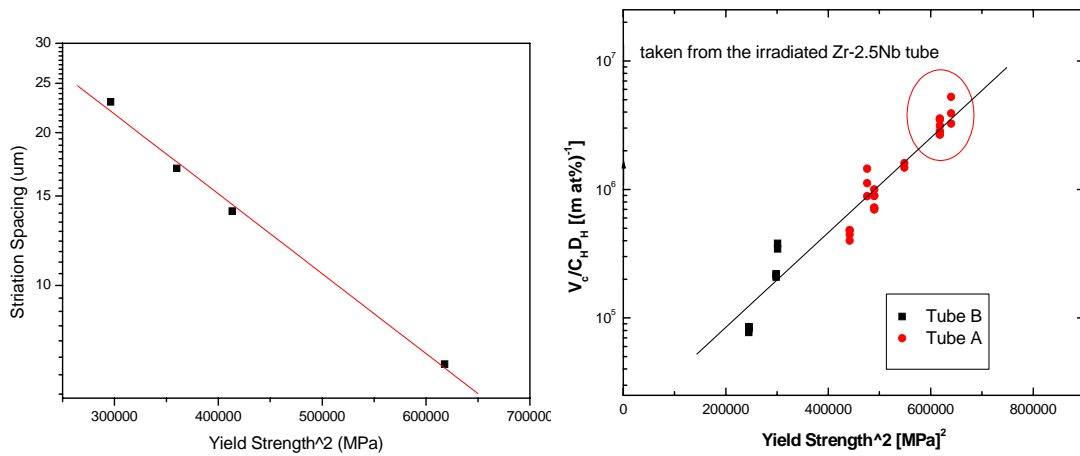


Fig. 6. Yield strength dependence of the striation spacing and the DHC velocity of the Zr-2.5Nb tube.

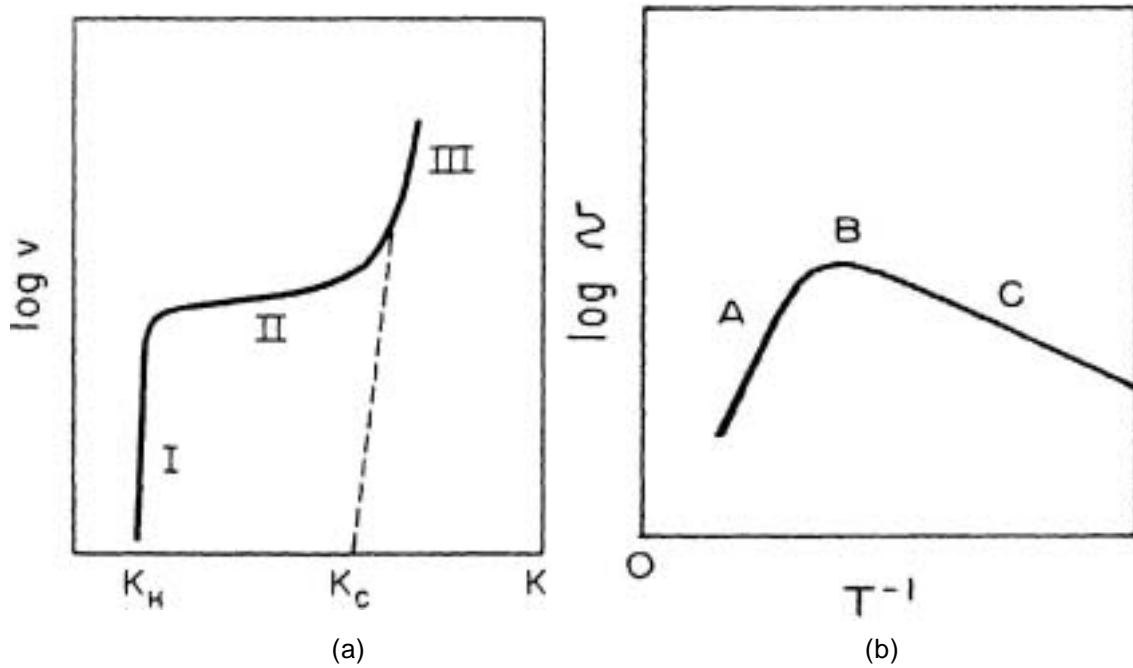


Fig. 7. Crack growth velocity as a function of applied stress intensity factor and temperature for steels exposed to hydrogen.

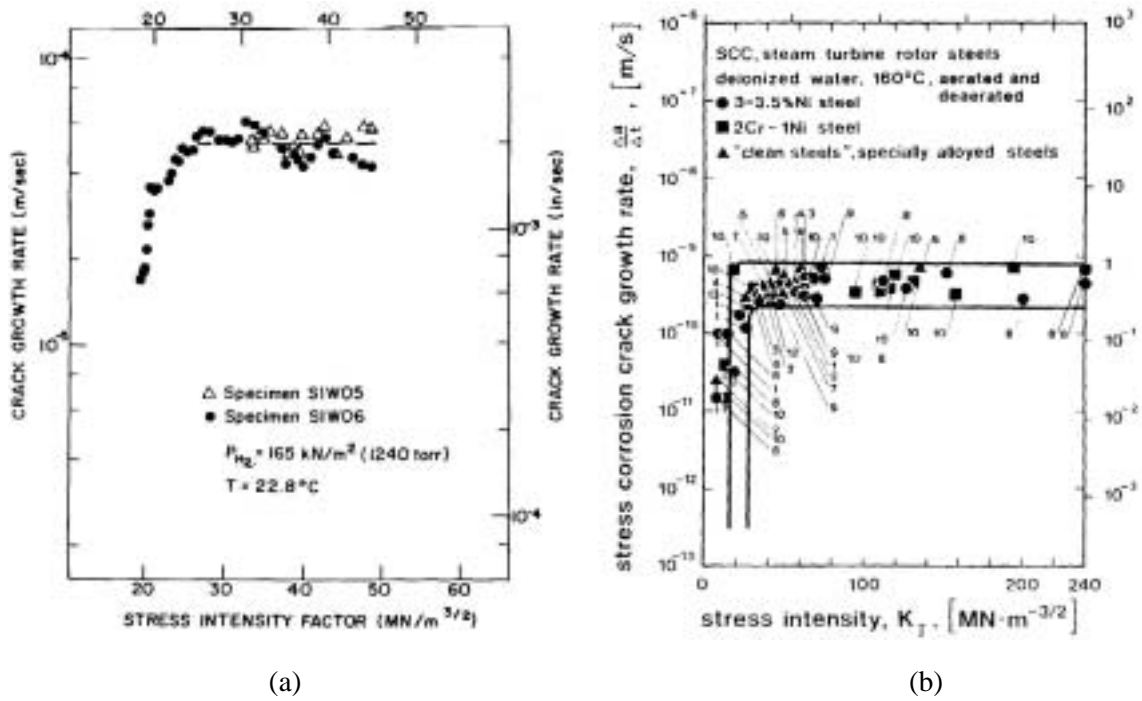


Fig. 8. (a) Crack growth rate of the 18 Ni maraging steel in 165 KN/m² at 23 °C and (b) SCC in steels exposed to water at 160 °C.

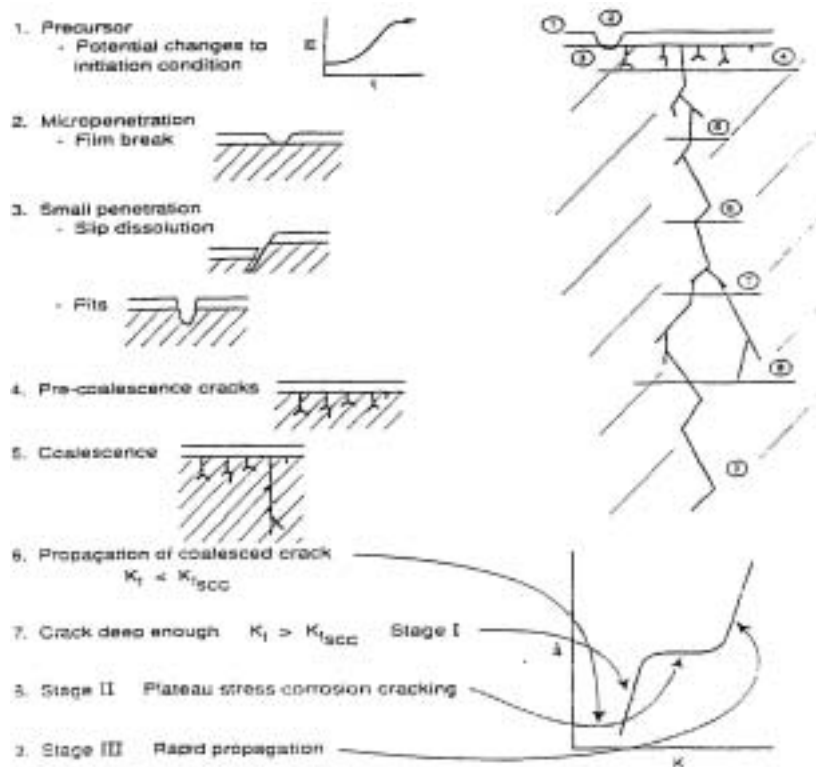


Fig. 9. Typical crack growth pattern and the correlation of the growth rate and applied stress intensity factor with the stages of the environmental assisted cracking of Ni-based alloys.

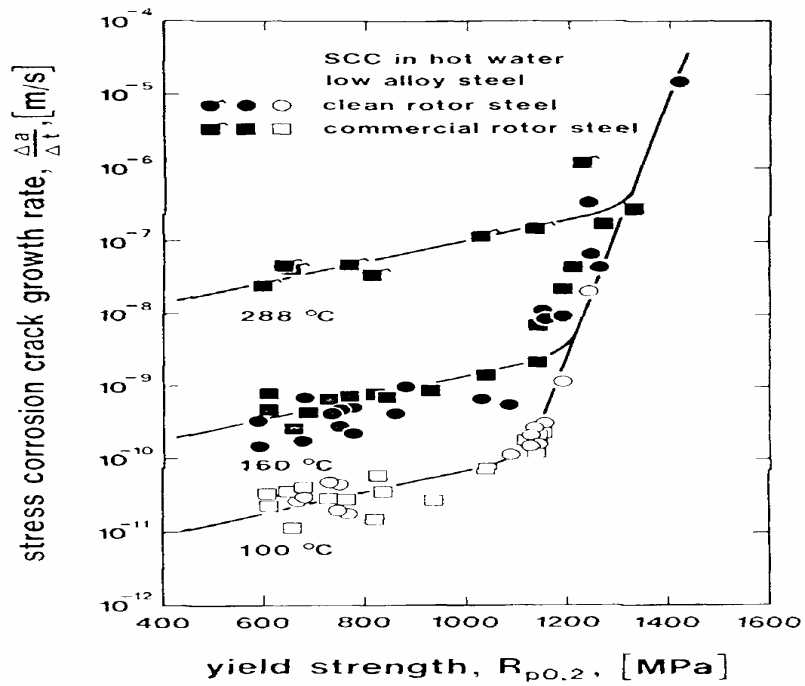


Fig. 10. Stress corrosion growth rate of steam turbine rotor steels with yield strength.

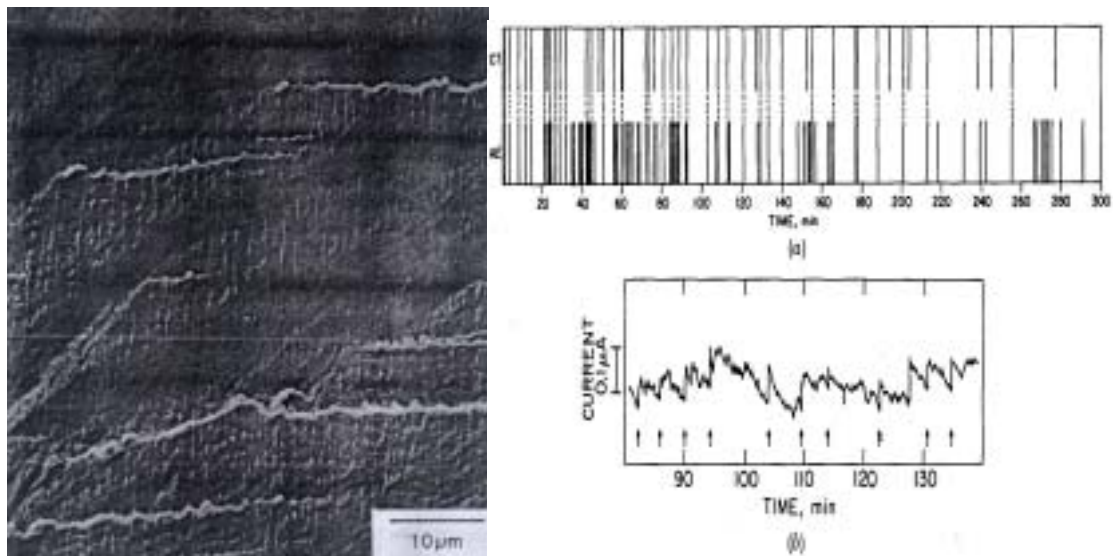


Fig. 11. Correlation of acoustic and electrochemical events for around 20 μm of decelerating crack growth in copper under constant displacement. The arrows indicate transients which had a very short rise time and were simultaneous with acoustic events.

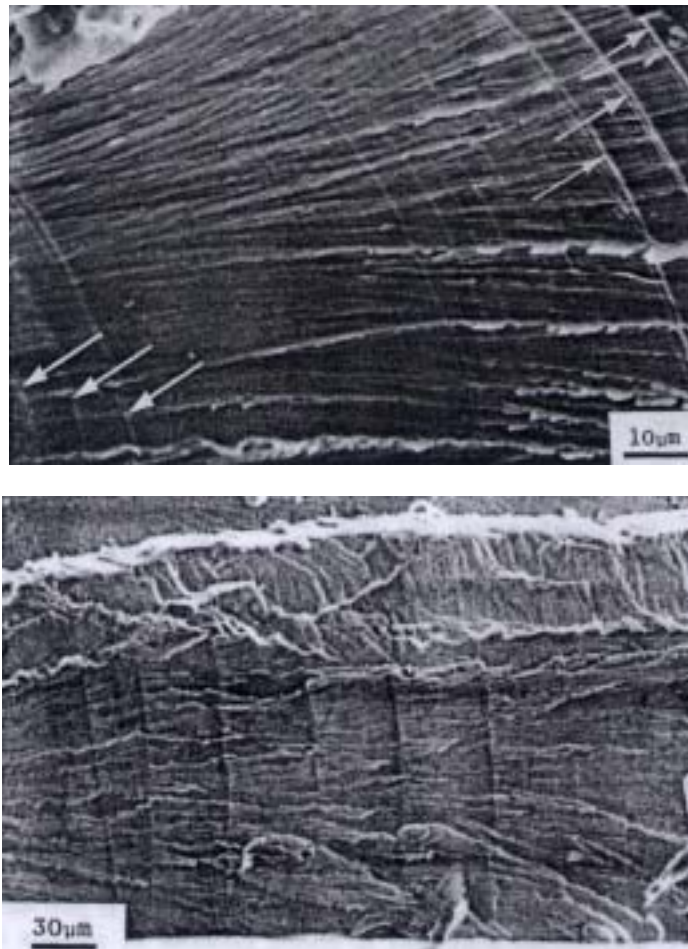


Fig. 12. Striation lines observed on the copper-based alloys after stress corrosion cracking tests.